Supporting Information

Phosphorus-triggered synergy of phase transformation and chalcogenide vacancy migration in cobalt sulfide for efficient oxygen evolution reaction

Suli Liu,[*a] Chenjing Che,[a] Haiyan Jing,[a] Jun Zhao,[a] Xueqin Mu,[a] Sudi Zhang,[a] Changyun Chen[a] and Shichun Mu[*b]

[a]Key Laboratory of Advanced Functional Materials of Nanjing, Nanjing Xiaozhuang University, Nanjing 211171, China. E-mail: niuniu_410@126.com.

[b]State Key Laboratory of Advanced Technology for Materials Synthesis and Processing, Wuhan University of Technology, Wuhan 430070, China. E-mail: msc@whut.edu.cn.

Characterization. X-ray diffraction (XRD) was used to measure the crystal structures. The morphologies of the developed catalyst were studied by TEM, and high-resolution TEM (HRTEM) and HAADF-STEM images. The elemental valence states of the catalysts were probed by the X-ray photoelectron spectroscopy (XPS) was carried out for chemical composition. For the test details, see our previous reports.

Electrochemical Tests

Electrochemical HER measurements. The electrochemical HER experiments were carried out using a CHI 660E electrochemical workstation (Shanghai, Chenhua Co.) with a standard three electrode system. A graphite rod and Ag/AgCl (3 M KCl) served as the counter electrode and reference electrode, respectively. All the potentials were referenced to a reversible hydrogen electrode (RHE). A glassy carbon electrode (3 mm in diameter) was used in the HER experiments. In 0.5 M H_2SO_4, all the potentials were referenced to a reversible hydrogen electrode (RHE) by adding a value of 0.21. In 1.0 M KOH, all the potentials were referenced to a reversible hydrogen electrode (RHE) by adding a value of 1.02.

Electrochemical OER measurements. Electrochemical experiments were performed on an Autolab electrochemical workstation (PGSTAT 302N, Metrohm, Netherlands). The glassy carbon electrode (5 mm in diameter) decorated by the samples were used as the working electrode, while Hg/HgO electrode and platinum sheet were applied as the reference electrode and counter electrode, respectively. Both potentials appearing in this paper transformed to vs RHE (reversible hydrogen electrode) and polarization curves were corrected concerning the iR compensation within the electrolyte. The values of potential vs RHE were calibrated by the $E_{vs.\ RHE} = E_{vs.\ Hg/HgO} + 0.098 + 0.0592 \times 13$. The polarization curves of as-prepared product were recorded at a sweep rate of 5 mV s^{-1} in 0.1 M or 1.0 M KOH solution after activation and cyclic stabilizing (a sweep rate of 50 mV s^{-1}).

Method and Model

The first principles calculations in the framework of density functional theory,

including structural, electronic performances, were carried out based on the Cambridge Sequential Total Energy Package known as CASTEP.[1] The exchange–correlation functional under the generalized gradient approximation (GGA)[2] with norm-conserving pseudopotentials and Perdew–Burke–Ernzerhof functional was adopted to describe the electron–electron interaction.[3] An energy cutoff of 750 eV was used and a k-point sampling set of 5 x 5 x 1 were tested to be converged. A force tolerance of 0.01 eV $Å^{-1}$, energy tolerance of $5.0x10^{-7}$eV per atom and maximum displacement of $5.0x10^{-4}$ Å were considered. The surfaces of Co_3O_4-P (100) $\{Co_{0.37}S_{0.38}P_{0.02}\}$ and Co_9S_8 (311) $\{Co_9S_8\}$ were built with the vacuum space along the z direction is set to be 15 Å, which is enough to avoid interaction between the two neighboring images. The top three atomic layers were relaxed and the bottom three atomic layers were fixed, then the intermediates have been absorbed on the surface of substrates.

Adsorption energy ΔE of A group on the surface of substrates was defined as:[4]

$$\Delta E = E_{*A} - (E_{*} + E_{A}) \quad (1)$$

where *A and * denote the adsorption of A group on substrates and the bare substrates, E_A denotes the energy of A group.

Gibbs free energy change (ΔG) of each chemical reaction is calculated by:

$$\Delta G = \Delta E + \Delta ZPE - T\Delta S \quad (2)$$

where E, ZPE, T and S denote the calculated total energy, zero point energy.

References

[1] M. D. Segall, P. J. D. L. M. J. Probert, C. J. Pickard, P. J. Hasnip, S. J. Clark and M. C. Payne, J. Phys.: Condens. *Matter*, **2002**, *14*, 2717.

[2] J. P. Perdew, K. Burke and M. Ernzerhof, *Phys. Rev. Lett.*, **1996**,*77*, 3865.

[3] D. R. Hamann, M. Schlüter and C. Chiang, Phys. *Rev. Lett.*, **1979**, *43*, 1494.

[4] Voiry, D.; Yamaguchi, H.; Li, J.; Silva, R.; Alves, D. C. B.; Fujita, T.; Chen, M. W.; Asefa, T.; Shenoy, V.; Eda, G.; Chhowalla, M. *Nat. Mater.* **2013**, *12*, 850-855.

Table S1. The elemental Co, P and S atomic percentage from ICP analysis for different samples

obtained by different phosphorization processes.

Sample	The amount of phosphorization	Formula
1	0	Co_9S_8
2	3	$Co_{0.58}S_{0.73}P_{0.01}$
3	5	$Co_{0.37}S_{0.38}P_{0.02}$
4	8	$Co_{0.70}S_{0.59}P_{0.16}$

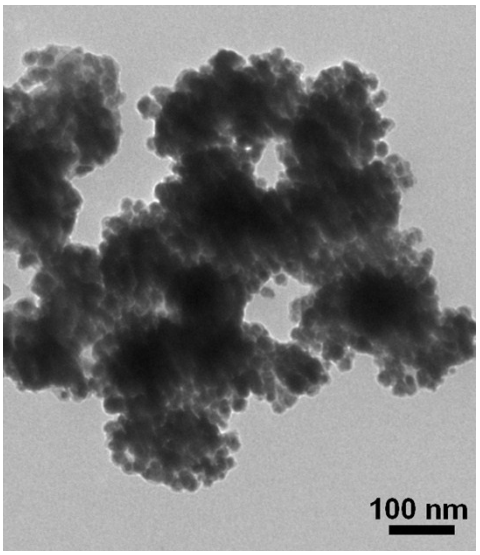

Fig. S1 TEM image of the as-prepared Co_9S_8 NPAs.

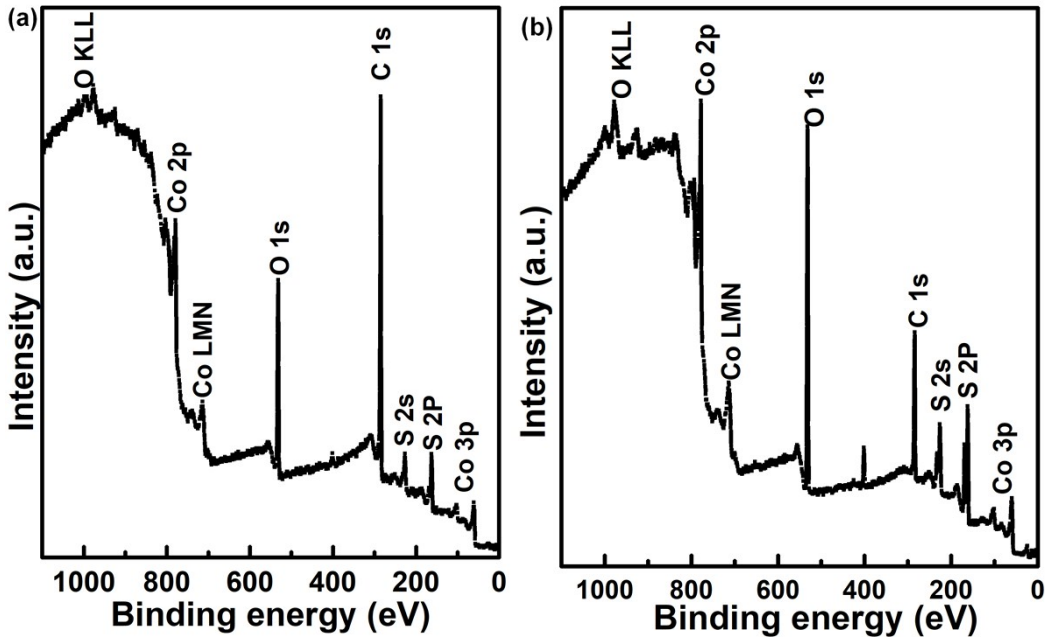

Fig. S2 XPS survey spectra of the (a) Co_9S_8 NPAs and (b) P-Co_3S_4 ($Co_{0.37}S_{0.38}P_{0.02}$) NSs synthesized under the typical reaction conditions.

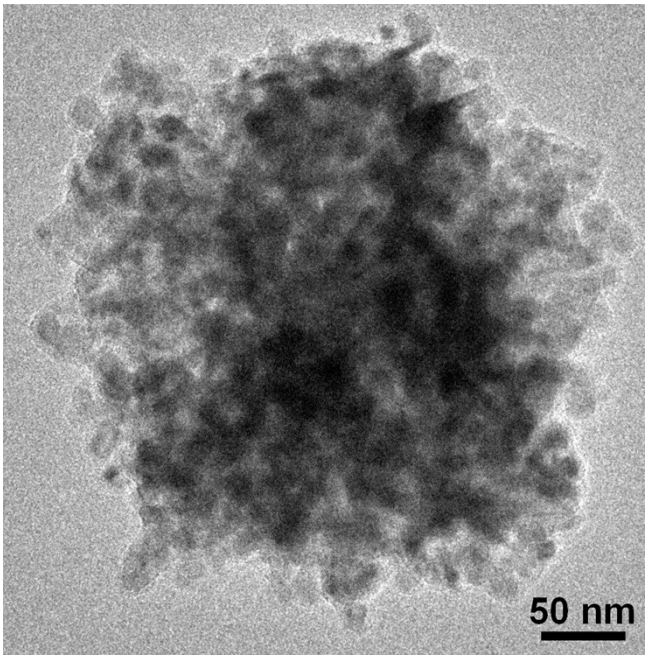

Fig. S3 High-resolution TEM image of the as-prepared Co_9S_8 NPAs.

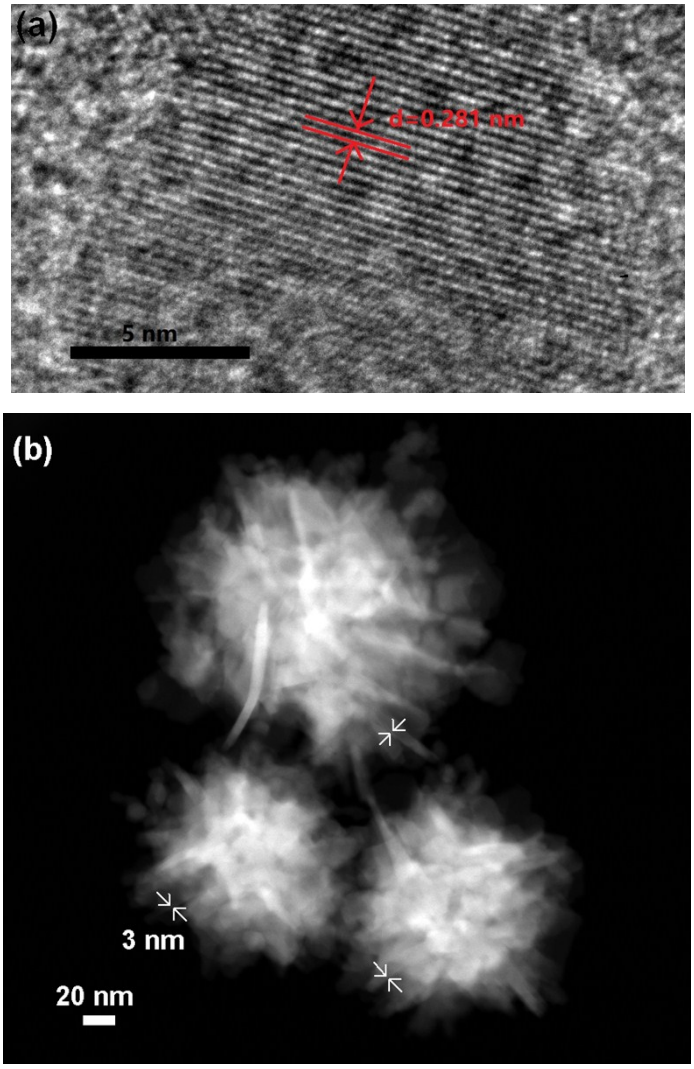

Fig. S4 (a) HRTEM image of the as-prepared Co_9S_8 NPAs. (b) HAADF-STEM image of $Co_{0.37}S_{0.38}P_{0.02}$.

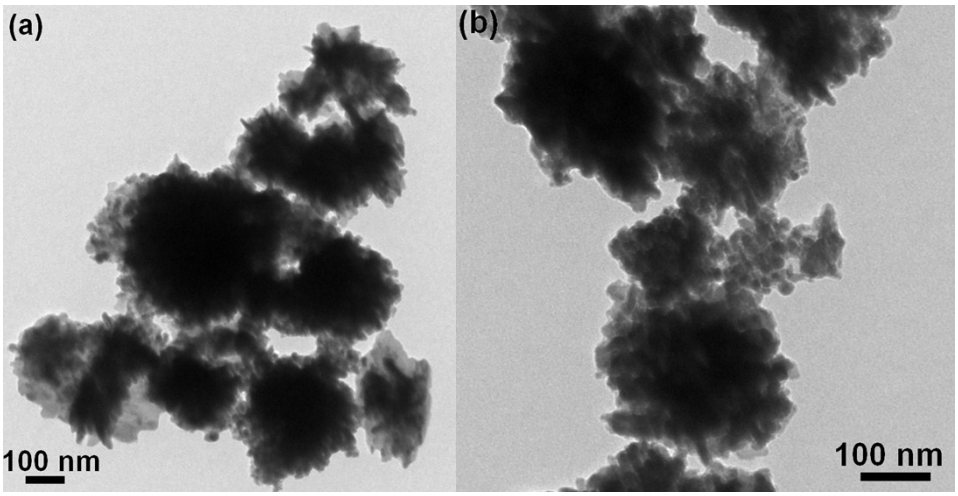

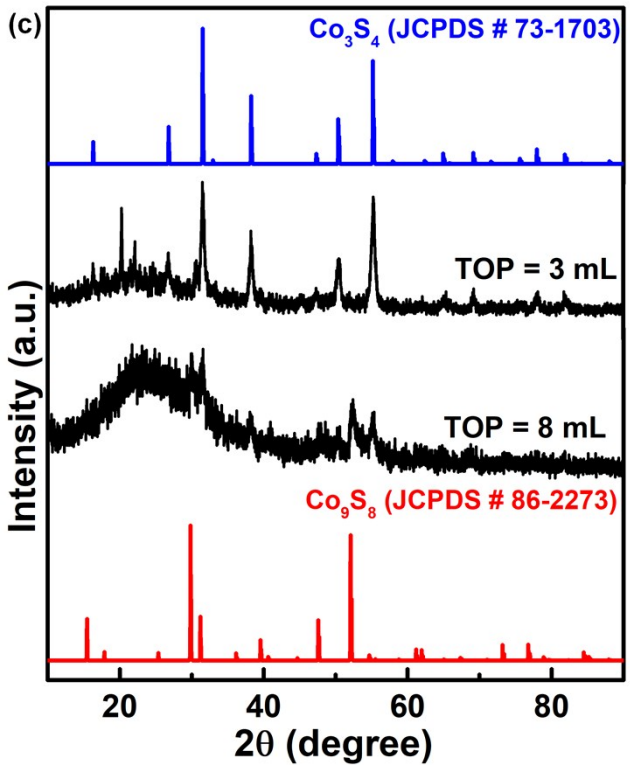

Fig. S5 Phase and morphology of the cobalt monophosphosulfides. TEM images of (a) $Co_{0.58}S_{0.73}P_{0.01}$ and (b) $Co_{0.70}S_{0.59}P_{0.16}$. (c) XRD pattern.

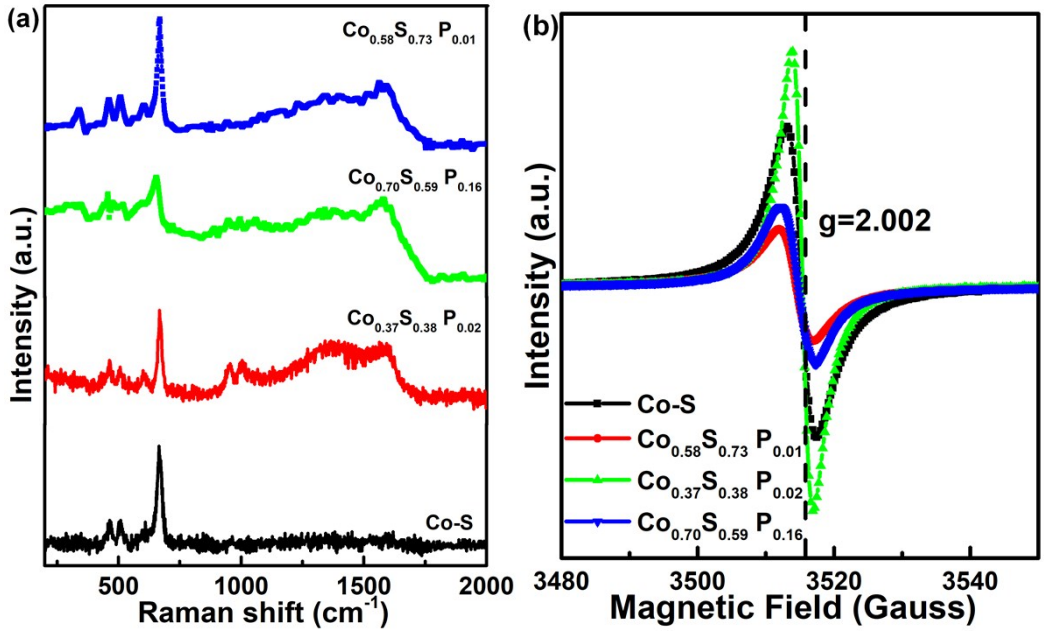

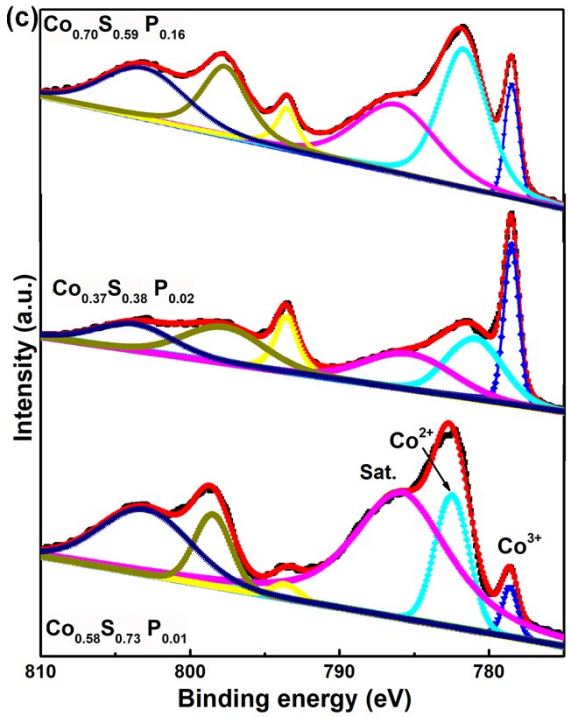

Fig. S6 (a) Raman spectra, (b) room-temperature EPR spectra, and (c) Co 2p XPS spectra of cobalt monophosphosulfides.

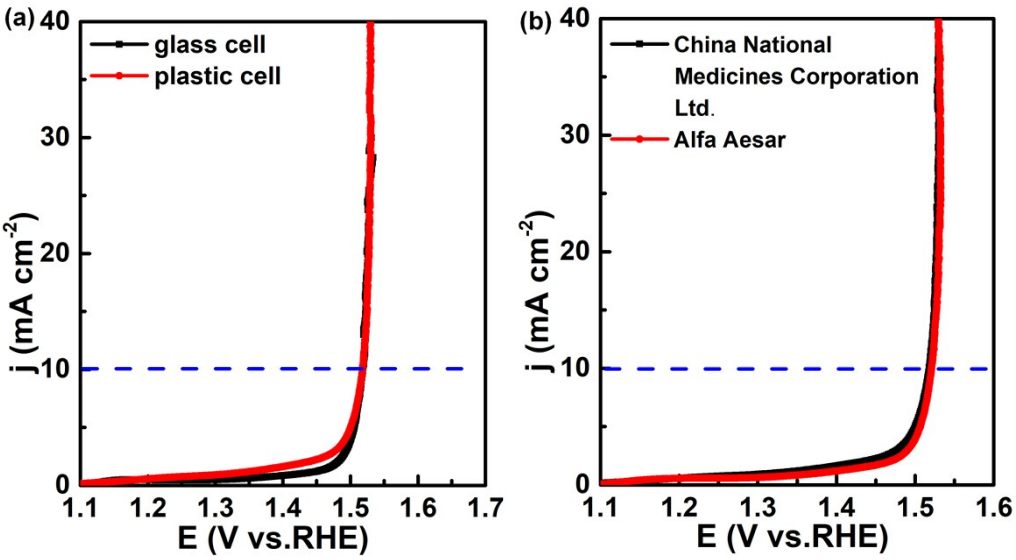

Fig. S7 (a) Polarization curves of $Co_{0.37}S_{0.38}P_{0.02}$ in 0.1 M KOH solution in a glass cell and plastic cell, respectively, at a scan rate of 5 mV s^{-1}. (b) Polarization curves of $Co_{0.37}S_{0.38}P_{0.02}$ in 0.1 M KOH solutions (Alfa Aesar and China National Medicines Corporation Ltd.) in plastic cells at a scan rate of 5 mV s^{-1}.

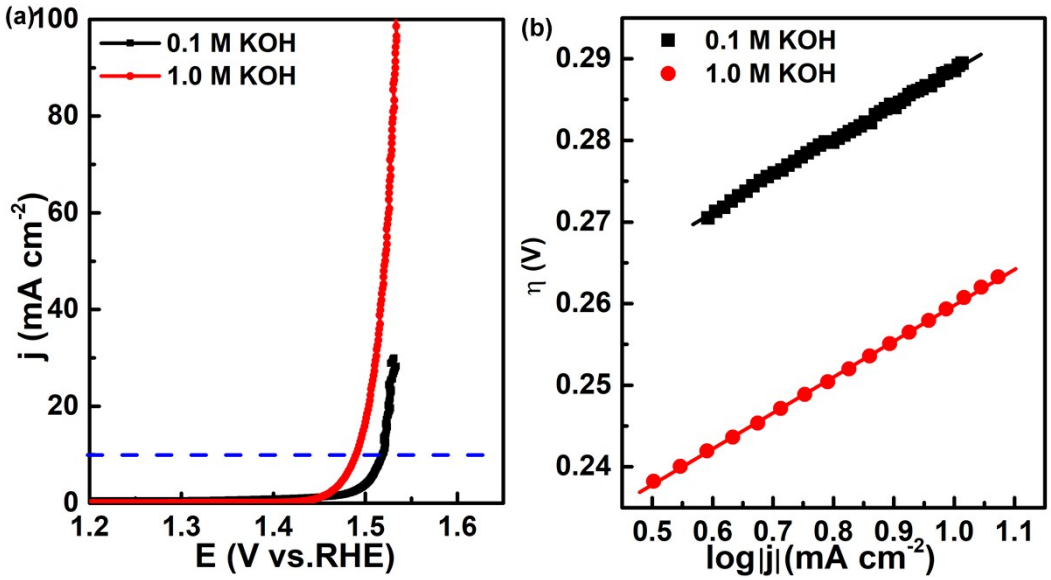

Fig. S8 (a) Polarization curves of $Co_{0.37}S_{0.38}P_{0.02}$ in 0.1 M KOH and 1.0 M KOH at a scan rate of 5 mV s^{-1}. (b) Corresponding Tafel plots.

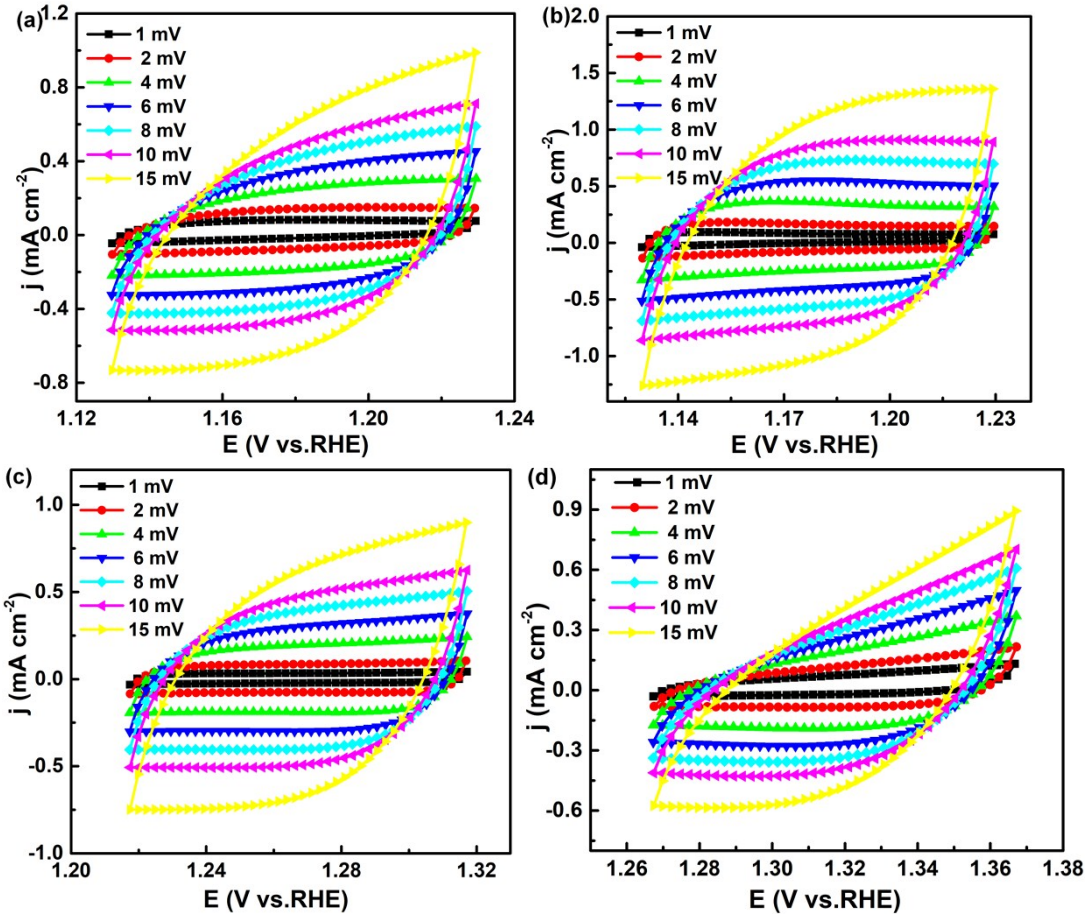

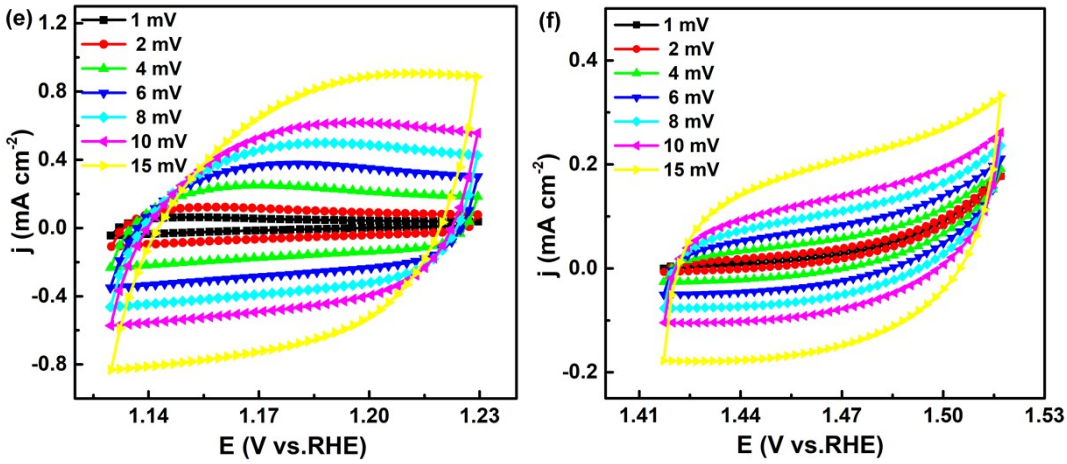

Fig. S9 CV curves of (a) $Co_{0.58}S_{0.73}P_{0.01}$, (b) $Co_{0.37}S_{0.38}P_{0.02}$, (c) $Co_{0.70}S_{0.59}P_{0.16}$, (d) Co-S, (e) Co-P, and (f) Co_3O_4 electrodes.

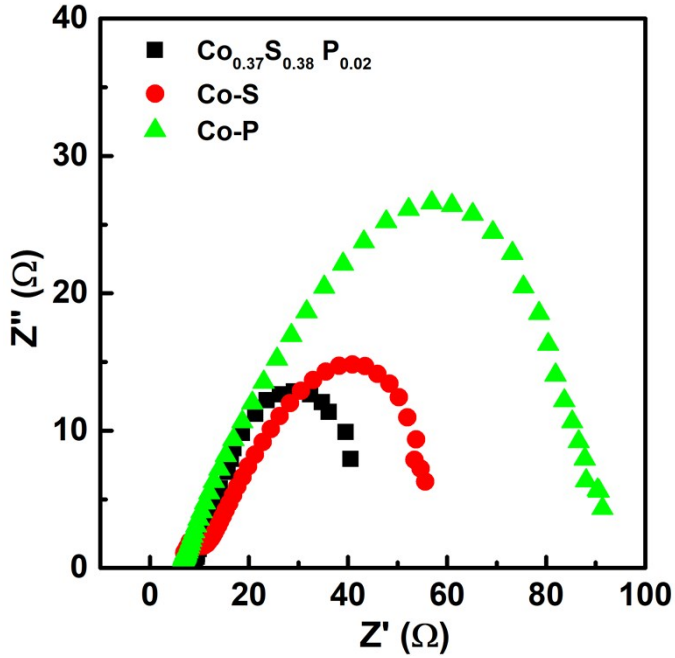

Fig. S10 the electrochemical impedance plots obtained at a potential of 1.63 V vs. RHE.

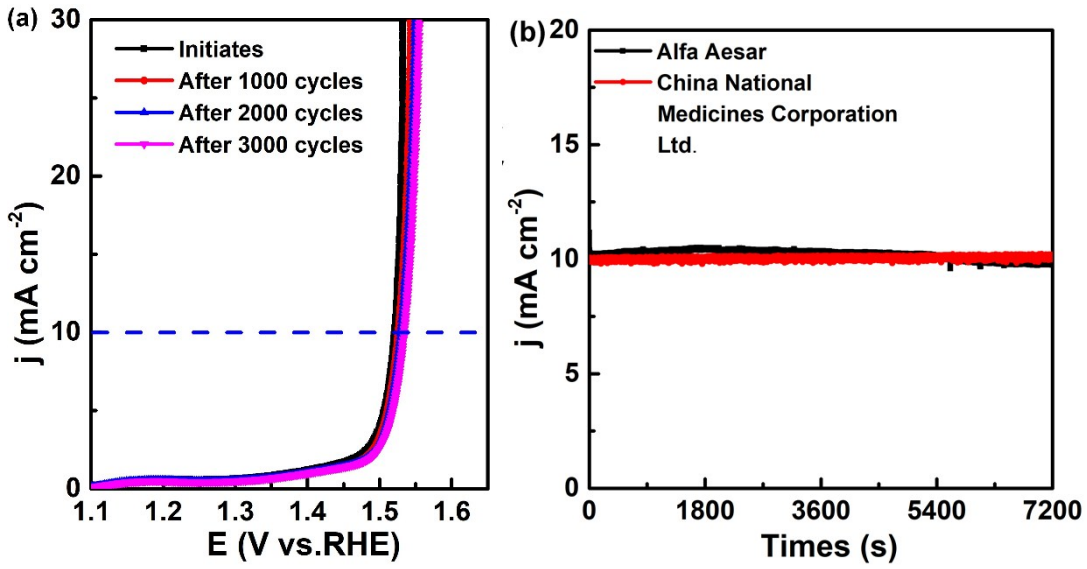

Fig. S11 (a) Polarization data for the $Co_{0.37}S_{0.38}P_{0.02}$ sample in 0.1 M KOH initially and after 1000, 2000, and 3000 CV sweeps between +1.1 and +1.6 V vs RHE in a 0.1 M KOH solution (Alfa Aesar) in a plastic cell. (b) The chronoamperometric curves of $Co_{0.37}S_{0.38}P_{0.02}$ at η_{10} (Alfa Aesar or China National Medicines Corporation Ltd.) in a 0.1 M KOH solution in a plastic cell.

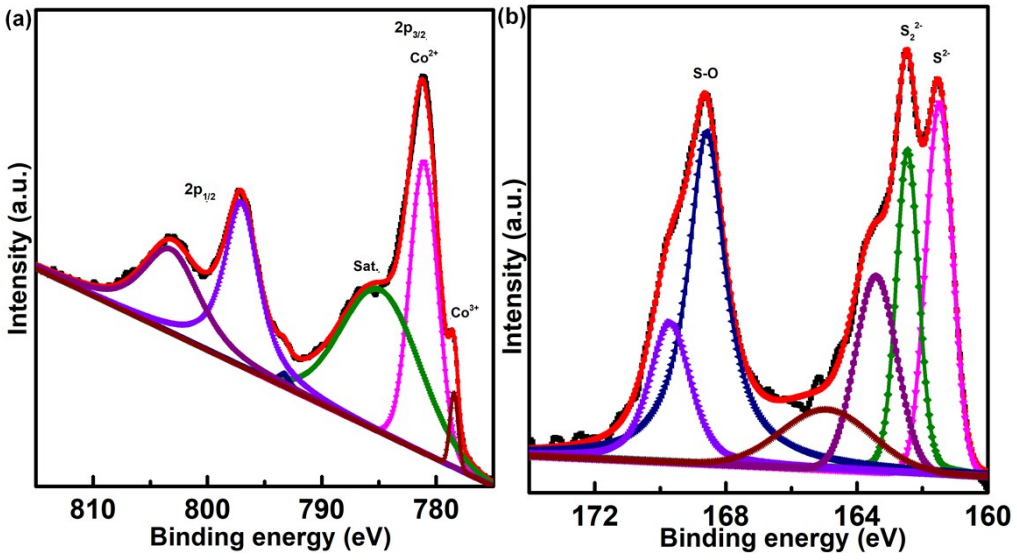

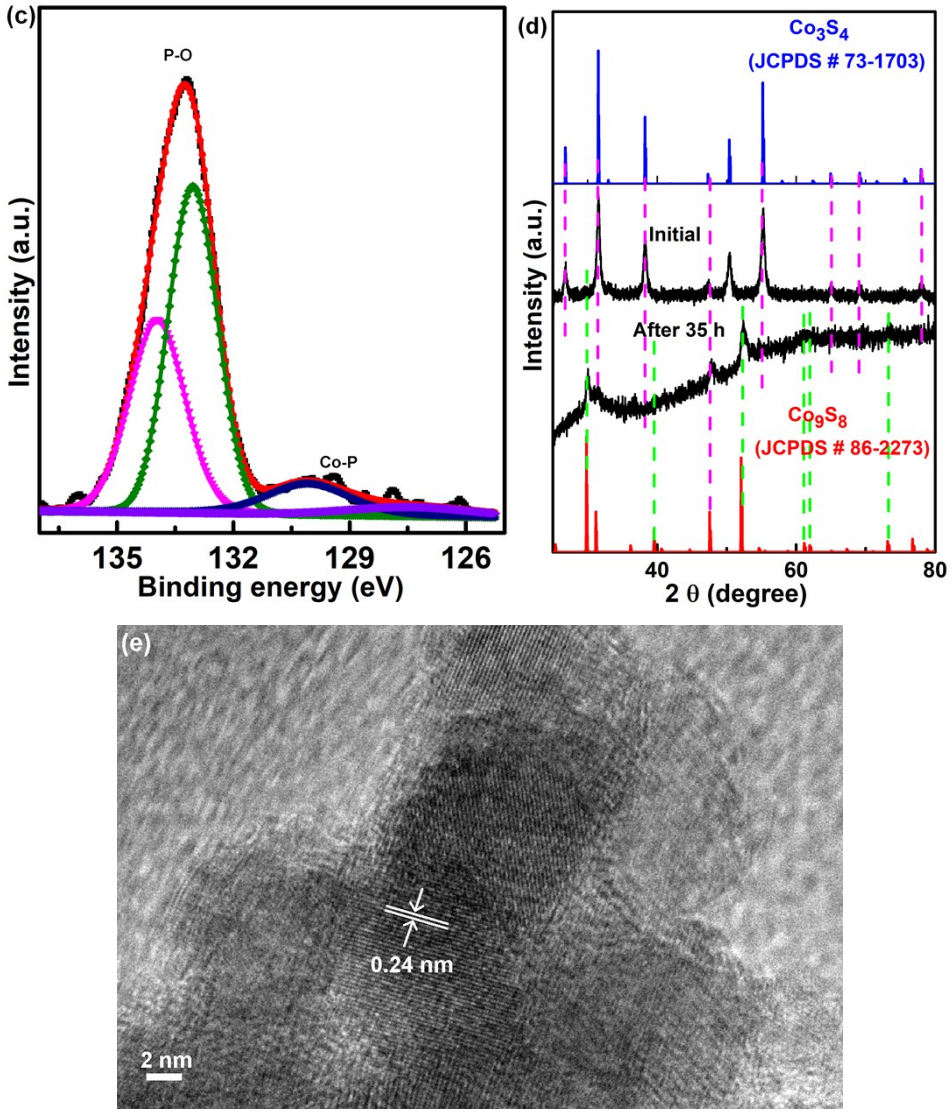

Fig. S12 XPS spectra of as-synthesized pyrite-structured $Co_{0.37}S_{0.38}P_{0.02}$ after the OER properties in 0.1 M KOH, (a) Co 2p, (b) S 2p, and (c) P 2p XPS spectra, respectively. (d) XRD pattern and (e) HRTEM image of $Co_{0.37}S_{0.38}P_{0.02}$ after the OER properties.

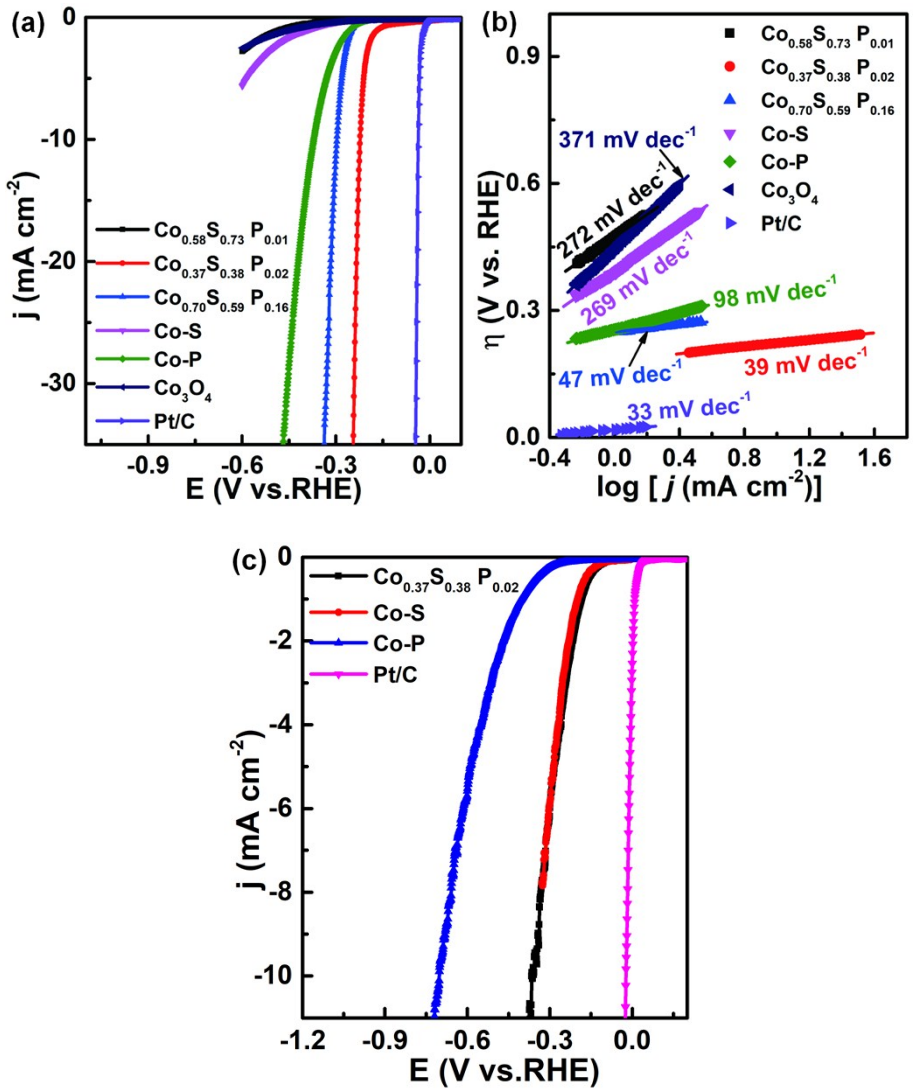

Fig. S13 (a) Polarization curves and (b) Tafel plots in 0.5 M H_2SO_4. (c) Polarization curves in 1.0 M PBS solution.

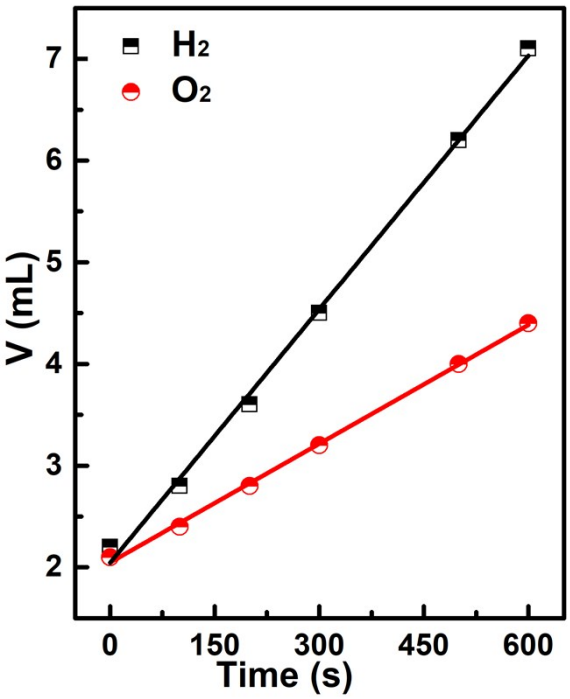

Fig. S14 the faradaic efficiency of $Co_{0.37}S_{0.38}P_{0.02}$.

Table S2. ICP analysis of KOH from Alfa Aesar and China National Medicines Corporation Ltd.

	element	content	unit		element	content	unit
Alfa Aesar	K	3402.7	mg/L	China National Medicines Corporation Ltd.	K	3424.3	mg/L
	Na	26.318	mg/L		Na	30.894	mg/L
	Si	0.3577	mg/L		Si	1.0822	mg/L
	W	0.1152	mg/L		W	0.1864	mg/L
	Sn	0.0649	mg/L		Ca	0.1309	mg/L
	Al	0.0475	mg/L		Al	0.1070	mg/L
	P	0.0199	mg/L		Sn	0.0852	mg/L
	Ta	0.0193	mg/L		Ba	0.0488	mg/L
	Ba	0.0154	mg/L		P	0.0177	mg/L
	Mo	0.0142	mg/L		B	0.0176	mg/L
	Sb	0.0132	mg/L		Mo	0.0174	mg/L
	Se	0.0122	mg/L		As	0.0165	mg/L
	Co	0.0073	mg/L		Ta	0.0164	mg/L
	Tl	0.0062	mg/L		Hg	0.0152	mg/L
	Au	0.0055	mg/L		Sb	0.0121	mg/L
	Ca	0.0052	mg/L		Pt	0.0114	mg/L
	Ir	0.0047	mg/L		Nb	0.0101	mg/L
	Pr	0.0041	mg/L		Fe	0.0090	mg/L
	Sm	0.0039	mg/L		Se	0.0060	mg/L
	Ge	0.0039	mg/L		Co	0.0054	mg/L
	B	0.0034	mg/L		Ni	0.0053	mg/L

Fe	0.0031	mg/L	Pb	0.0053	mg/L
Ga	0.0031	mg/L	Tl	0.0041	mg/L
Zn	0.0030	mg/L	Pr	0.0040	mg/L
Pt	0.0029	mg/L	Sm	0.0035	mg/L
S	0.0029	mg/L	Sr	0.0032	mg/L
Mg	0.0029	mg/L	Nd	0.0027	mg/L
Pb	0.0024	mg/L	Ga	0.0026	mg/L
Cu	0.0023	mg/L	Te	0.0025	mg/L
Hf	0.0022	mg/L	Li	0.0025	mg/L
In	0.0022	mg/L	Cr	0.0024	mg/L
Cr	0.0021	mg/L	Mg	0.0024	mg/L
Nd	0.0017	mg/L	In	0.0020	mg/L
Y	0.0015	mg/L	S	0.0018	mg/L
Ce	0.0014	mg/L	Hf	0.0016	mg/L
As	0.0014	mg/L	Y	0.0015	mg/L
Te	0.0013	mg/L	Ti	0.0015	mg/L
Mn	0.0013	mg/L	Bi	0.0014	mg/L
Be	0.0012	mg/L	Lu	0.0014	mg/L
Ru	0.0012	mg/L	Ru	0.0014	mg/L
Eu	0.0012	mg/L	Zn	0.0013	mg/L
Sr	0.0011	mg/L	Be	0.0012	mg/L
Ti	0.0011	mg/L	Au	0.0012	mg/L
Rh	0.0011	mg/L	Gd	0.0012	mg/L
Lu	0.0011	mg/L	Tb	0.0012	mg/L
Nb	0.0010	mg/L	Ge	0.0012	mg/L
Er	0.0009	mg/L	Mn	0.0011	mg/L
Li	0.0008	mg/L	Zr	0.0011	mg/L
Hg	0.0007	mg/L	Eu	0.0011	mg/L
Sc	0.0007	mg/L	Pd	0.0009	mg/L
Bi	0.0007	mg/L	Cu	0.0008	mg/L
Ho	0.0006	mg/L	Rh	0.0007	mg/L
Gd	0.0006	mg/L	Dy	0.0007	mg/L
Ag	0.0006	mg/L	Sc	0.0007	mg/L
Yb	0.0004	mg/L	V	0.0006	mg/L
Tm	0.0004	mg/L	Tm	0.0005	mg/L
V	0.0004	mg/L	Ce	0.0005	mg/L
Pd	0.0004	mg/L	Ir	0.0004	mg/L
Zr	0.0003	mg/L	Cd	0.0004	mg/L
Dy	0.0003	mg/L	Yb	0.0003	mg/L
Tb	0.0002	mg/L	Ho	0.0001	mg/L
Cd	0.0002	mg/L	Ag	0.0001	mg/L
La	0.0001	mg/L	Er	0.0001	mg/L
Ni	0.0001	mg/L	La	0.0001	mg/L

Table S3. Comparison of OER activities of metal sulfides and phosphides catalysts in alkaline condition.

Materials	η_{10} (mV)	Electrolyte	Tafel slope (mV dec^{-1})	Ref.
$Co_{0.37}S_{0.38}P_{0.02}$ NSs	288	0.1 M KOH	43.4	This work
$Co_{0.37}S_{0.38}P_{0.02}$ NSs	257	1.0 M KOH	44.0	This work
CoP	320	1.0 M KOH	71	*ACS Catal.* 2015, 5, 6874.
$NiMoP_2$	330	1.0 M KOH	90.6	*J. Mater. Chem. A* 2017, 5, 7191.
$CoS_{4.6}O_{0.6}$	290	1.0 M KOH	67	*Angew. Chem. Int. Ed.* 2017, 56, 4858-4861
Co_3S_4 nanosheets	355	1.0 M KOH	48	*Angew. Chem. Int. Ed.* 2015, 54, 11231.
CoP_3/NAs/CFP	334	1.0 M KOH	62	*J. Mater. Chem. A* 2016, 4, 14539.
CoS_2 (400)/N,S-GO	390	0.1 M KOH	75	*ACS Catal.* 2015, 5, 3625.
N-Co_9S_8/graphene hybrid	409	1.0 M KOH	82.7	*Energy Environ. Sci.* 2016, 9, 1320.
Co_3S_4@MoS_2	280	1.0 M KOH	43	*Nano Energy* 2018, 47, 494.
CoP NR/C	360	0.1 M KOH	66	*ACS Catal.* 2015, 5, 4066.
Co@MoS_2	270	1.0 M KOH	74	*Nanoscale* 2017, 9, 2711.
Co/Co_2P	390	1.0 M KOH	59.8	*ACS Energy Lett.* 2016, 1, 1192.
$Co_{0.9}S_{0.58}P_{0.42}$	266	1.0 M KOH	48	*ACS Nano* 2017, 11, 11031-11040.
Co/Co_xM_y	334	1.0 M KOH	/	*Small* 2019, 12, 1901518.
Co-P film	345	1.0 M KOH	47	*Angew. Chem. Int. Ed.* 2015, 54, 6251.
Se/Ni-Co_3O_4	290	1.0 M KOH	62.9	*ACS Sustainable Chem. Eng.* 2019, 7, 11901.
$Co_xNi_{1-x}Fe_2O_4$	381	1.0 M KOH	46.4	*ACS Appl. Mater. Interfaces* 2017, 9,

13132.

Table S4. Comparison of HER activities of metal sulfides and phosphides catalysts in 1.0 M KOH.

Materials	η_{10} (mV)	Tafel slope (mV dec^{-1})	Stability (h)	Ref.
$Co_{0.37}S_{0.38}P_{0.02}$ NSs	218	103	35	This work
Ni_9S_8	230	123	24	*Adv. Funct. Mater.* 2016, *26*, 3314.
PNC/Co	298	131	10	*J. Mater. Chem. A* 2016, *4*, 3204.
MoS_2/NiS	244	97	12	*Small* 2018, 1803639.
CoS_x/Ni_3S_2@NF	204	133.32	20	*ACS Appl. Mater. Interfaces* 2018, 1033, 27712.
Co-Fe binary oxide composite	220	51		*Catal. Today* 2019, *doi.org/10.1016/j.cattod.2019.01.060*
MoS_2-3	201	118	24	*Chem. Eur. J.* 2018, 24, 19075.
FeP nanorod arrays/carbon cloth	218	146	20	*ACS Catal.* 2014, 4, 4065.
CoP/CC	209	129	22	*J. Am. Chem. Soc.* 2014, 136, 7587.
NiMo MT/NF	119	119	10	*Int. J. Hydrogen Energy* 2019, 44, 24712.
$CoS_{1.097}/MoS_2$	249	75	21	*ACS Appl. Energy Mater.* 2019, 2, 10, 7504.
MoS_2/CNT-graphene	255	100		*Nat. Mater.* 2016, 15, 1003.

Ni@C 400 NSs	270	143		*J. Mater. Chem. A*. 2017, 5, 17954.
$NiCo_2S_4$/NF	248	113.7	12	*ACS Appl. Mater. Interfaces*. 2017, 9, 15364.

Table S5. Overall water splitting activity comparison for catalysts in this work with previously reported ones in alkaline solution.

Materials	Voltage (V) at 10 mA cm^{-2}	Electrolyte	Substrate	Ref.
$Co_{0.37}S_{0.38}P_{0.02}NS_S$	1.59	1.0 M KOH	Ni foam	This work
Pt/C-RuO_2	1.63	1.0 M KOH	Ni foam	*ACS Appl. Mater. Interfaces* 2019, 11, 6890.
$P_{8.6}$-Co_3O_4/NF	1.63	1.0 M KOH	Ni foam	*ACS Catal.* 2018, 8, 2236.
Pt/C-IrO_2	1.58	1.0 M KOH	Ni foam	*Adv. Energy Mater.* 2017, 7, 1602122.
Co_xPO_4/CoP	1.91	1.0 M KOH	- -	*Adv. Mater.* 2015, 27, 3175.
$NiCo_2O_4$	1.65	1.0 M NaOH	Ni foam	*Angew. Chem. Int. Ed.* 2016, 55, 6290.
Co@Co_3O_4-NC	2.00	1.0 M KOH	Ni foam	*J. Mater. Chem. A* 2017, 5, 9533.
p-$CoSe_2$/CC	1.62	1.0 M KOH	Ni foam	*ACS Sustainable Chem. Eng.* 2018, 6, 15374.
Co-P	1.65	1.0 M KOH	Cu foil	*Angew. Chem., Int. Ed.* 2015, 54, 6251.
NiS/Ni_2P/CC	1.67	1.0 M KOH	carbon cloth	*ACS Appl. Mater. Interfaces* 2018, 105, 4689.
CoP@NPCP	1.66	1.0 M KOH	carbon paper	*Carbon* 2019, 150, 446.
CoPS	1.75	1.0 M KOH	Al_2O_3-3 electrode	*ACS Sustainable Chem. Eng.* 2018, 68, 10087.
P-Co-Ni-S/NF	1.60	1.0 M KOH	Ni foam	*ACS Appl. Mater. Interfaces* 2018, 108, 7087.